Current Research in Food Science 5 (2022) 892–903

Contents lists available at ScienceDirect

Current Research in Food Science

journal homepage: www.sciencedirect.com/journal/current-research-in-food-science

Particle filled protein-starch composites as the basis for plant-based meat analogues

Stacie Dobson [a], Thamara Laredo [b], Alejandro G. Marangoni [a,*]

[a] Department of Food Science, University of Guelph, 50 Stone Rd E, Guelph, Ontario, N1G 2W1, Canada
[b] Department of Chemistry, Lakehead University, 500 University Ave., Orillia, Ontario, L3V 0B9, Canada

ARTICLE INFO

Editor name: Patrick Ruhs

Keywords:
Waxy maize
Rapid swelling starch
Pea protein isolate
Particle filled matrix

ABSTRACT

Rapid swelling, high amylopectin starches including Thermally Inhibited (TI), Chemically Modified (CM), and Granular Cold- Swelling (GCS) were assessed for their supporting matrix forming potential and properties. Starches displayed identical calorimetric profiles with no endothermic events, and completely amorphous structure as judged by powder X-ray diffraction. However, they each provided different textural attributes. The starches were combined with pea protein isolate at a total concentration of 47%w/w (d.b.) to create a proteinacious supporting matrix. The starch protein matrix was then tested in a non-cold-set dough state as well as in a cold-set state after storage for 24h at 5°C. In the non-cold-set state, hardness increased with the addition of protein. CM was the softest dough and was difficult to work with, while TI and GCS were harder, with TI having the greatest resilience. Once cold-set, the textural properties changed, and GCS was not able to form a solid structure, instead remaining a viscoelastic dough. The hardness and storage modulus (G') of TI and CM displayed a negative correlation with the addition of protein due to matrix disruption. However, the combination of TI starch and pea protein at a ratio of 70% starch and 30% protein in the dry fraction displayed a synergistic effect, with increased resilience, chewiness, and ductility. FTIR of TI starch and protein at the same 70:30 ratio provided further evidence for the existence of an interaction between pea protein and TI starch. The results support the use of TI rapid swelling starch and pea protein isolate as a supporting matrix for application in meat analogue systems.

1. Introduction

Proteins and polysaccharides are essential macromolecules that are responsible for a variety of properties in food systems including, taste, texture, emulsion stability, and nutrition. Their role in plant-based food systems has become of great interest as the products created are highly dependent on the ability of the ingredients to form a complex structure and interact.

Animal-based products are environmentally harmful and unsustainable food sources, and associated with the food sector, are several ethical quandaries regarding the care and consumption of these animals and their products (De Bakker and Dagevos, 2012; Hampton et al., 2021) Along with the health benefits of following vegan and vegetarian diets, there has been a shift to using more sustainable ingredients and consuming plant-based foods. Meat analogues are an environmentally friendly alternative to meat, the products are plant-based, can provide similar nutritional protein value, and have smaller environmental impacts (Nijdam et al., 2012). However, most of the products on the market do a poor job at mimicking the actual fibrous texture of meat and instead consist of pressed patties and aggregated grounds (V. Joshi and Kumar, 2015). The products that do have a fibrous structure need to be manufactured using processes governed by high temperatures and high pressure, such as high-moisture extrusion and shear cell processing. These systems are not only costly but there are concerns with the quality of the proteins after this extensive processing (Alam et al., 2016).

There is a gap in the market for a filamentous meat analogue that can be created using simpler manufacturing processes, which are more sustainable, but can still mimic the functional structure of whole muscle animal meat.

Plant protein and starch are two of the most common ingredients in plant-based foods, and many investigations on their interactions have been carried out. However, the majority of the investigations use a combination of native starch and protein (Bühler et al., 2022; Donmez et al., 2021; M. Joshi et al., 2014; J.-Y. Li et al., 2006; Loveday, 2020;

* Corresponding author.
E-mail address: amarango@uoguelph.ca (A.G. Marangoni).

https://doi.org/10.1016/j.crfs.2022.05.006
Received 29 December 2021; Received in revised form 3 May 2022; Accepted 18 May 2022
Available online 27 May 2022

Ribotta et al., 2007; Ryan and Brewer, 2007; J. Wang et al., 2021). In all reported methods, starch and protein are in solution and require a heating step to induce either gelatinization of starch, or denaturation of the protein, followed by a setting period to create a self-supporting matrix. Ribotta et al. (2007) performed texture profile analysis and reported gel matrix weakening with the addition of soy protein, possibly due to the formation of hydrogen bonds with the starch. Joshi et al., studied lentil starch and lentil protein gels demonstrating that the ratio of starch to protein can influence gelation and physical behaviour. The magnitude of the storage modulus (G') was greater in higher starch containing gels than in protein-rich gels, indicating that starch provided the solid-like behavior (M. Joshi et al., 2014). While these results are promising, as starches and proteins can form unique complexes, the requirement for high-temperature heating to reach the gel state and for the matrix to initially behave like a viscous solution limits the application to certain food systems.

Through chemical and physical modification, starches can be altered to have better-suited functional properties (Majzoobi et al., 2015; Xiong and Fei, 2017). Chemical modification can add additional functional groups or covalent crosslinking between chains to strengthen the bonds and change the behavior of the starches increasing their resistance to saline and acidic environments (Neelam et al., 2012; Xiong and Fei, 2017). Physical modifications include those of pregelatinized and granular cold swelling starches. These forms of modification result in starches with rapid swelling capabilities. To prepare pregelatinized starches, native starch slurries can undergo drum drying, spray drying or extrusion to induce gelatinization, and thus loss of crystallinity (Ashogbon and Akintayo, 2014; Xiong and Fei, 2017). Granular cold swelling starches are made by heating the native starches in ethanolic solutions to remove the crystallinity but keep the outer granular structure (Majzoobi et al., 2015; Xiong and Fei, 2017). This results in increased cold temperature viscosity and better cold gel texture versus typical pregelatinized starch. However, many applications need even greater instant viscosity and better resistance to heat and acid. In this case, one can pregelatinize the chemically modified starches, though this can cause problems when attempting to classify this starch as clean label. Thermally inhibited starches are an exception to this. Thermally inhibited pregelatinized starches have properties similar to chemically cross-linked starches, but instead of added chemicals, the native starch is dehydrated extensively under alkaline conditions and subsequent dry heating (Neelam et al. 2012; Shah et al., 1998). The resulting starch is classified as thermally inhibited and becomes pregelatinized to create a clean label "functional native" starch that can be highly viscous and highly resistant to processing conditions (De Castro and Marketing Manager, 2015; M. Shah et al., 1998).

Pregelatinized starches have been investigated in gluten-free bread systems for their ability to form viscoelastic doughs (Onyango et al., 2011). Waxy maize starches are often used, as they have structural characteristics that allow rapid swelling, forming stringy and cohesive pastes (Onyango et al., 2011; Tattiyakul and Rao, 2000). However, the doughs tend to be supplemented by hydrocolloids, cereal flours, and native starch to improve the textural properties of the doughs as well as of the final baked product (Lazaridou et al., 2007; Mariotti et al., 2009).

For applications in a meat analogue, there has been limited research on the incorporation of rapid swelling starches. It has been observed that prolamin proteins such as zein, kafirin and hordein can have viscoelastic properties and form fibers, but these fibers alone, cannot match the textural properties of meat (Mattice and Marangoni, 2020a, 2020b; Oguntoyinbo et al., 2018; Taylor and Taylor, 2018; Y. Wang and Chen, 2012). A base material is needed to support the system, for which, to the best of our knowledge, only plant protein gels have been investigated, and processing limitations were identified (Mattice and Marangoni, 2020a).

In this research, however, the idea is to investigate rapid swelling starch as the base material to act as instantaneous support matrix for protein particles and the rest of the ingredients. The use of waxy starch in the supporting matrix would provide viscoelasticity to enable simultaneous elongation and separation of prolamin fibrils with the prospect creating a fine fibril network. However, the properties of a starch-only system would lack both the rheological, mechanical and nutritional properties associated with "meat". By incorporating protein isolate flours in the matrix, we create a particle filled network. Particle filled networks have been extensively explored and show that through modulation of the filler content, changes in the textural properties are observed and one can deduce information on matrix-filler interactions (Gravelle et al., 2015, 2017, 2019; Gravelle and Marangoni, 2021). By treating the supporting matrix as a particle-filled matrix, we can increase the protein content and modulate the mechanical properties of the starch-based embedding polymer matrix, without relying on the physical state or chemical nature of the protein.

Our objective is to create a starch matrix filled with protein particles and fibers, as a universal approach to creating plant-based meat analogues. We will test various waxy maize-based rapid swelling starches, including Chemically Modified (CM), Granular Cold-Swelling (GCS), and Thermally Inhibited (TI), in conjunction with pea protein isolate to develop a protein-starch dough complex with specific mechanical and rheological properties. The ratio of starch to protein will be adjusted, and the resulting changes will be measured through textural, rheological, and molecular analysis to provide information as to the interactions occurring within the system. These interactions could then be exploited to create a plant-based meat matrix with mechanical properties more closely resembling those of animal meat, without the need for extrusion.

2. Materials and methods

2.1. Materials

Pea protein isolate - obtained from Roquette (Roquette, Canada Ltd., MA, CA), Rapid swelling waxy maize starches - thermally inhibited, granular cold-water swelling, and chemically modified-via crosslinking - were all obtained from Ingredion (Ingredion Canada Inc. Mississauga, ON, CA).

2.2. Methods

2.2.1. Differential Scanning Calorimetry

The presence of crystallinity in starch was investigated using Differential Scanning Calorimetry (DSC) (Mettler Toledo, ON, Canada), Approximately 10 mg of appropriately hydrated starch was weighed into 30 μL aluminum pans and hermetically sealed to avoid water loss. The thermal analysis was performed over a temperature range of 30–100^{o}C and a heating rate of 5 ^{o}C/min. All samples were analyzed in at least duplicate. STAR software was used to investigate the thermograms for any potential peaks.

2.2.2. X-ray Diffraction

The crystal structure of starch was investigated using powder X-ray diffraction (Multiflex Powder XRD, Rigaku Corporation, Japan) The X-ray source was a copper x-ray tube operated at 40 kV and 44 mA. The scan rate was 0.05^{o} per sec over a range of 1^{o} to 30^{o}. Jade9 software was used to analyze the data.

2.2.3. Microscopy

Starch samples were investigated using bright field and polarized light microscopy (M838PL-C180U3, OMAX; Kent, WA, USA). Starch suspensions were placed onto glass microscope slides and covered with a coverslip. Iodine stain solution was then placed on the edge of the coverslip to slowly stain the starch suspension. Images were captured in both bright field and under polarized light using an 18 MP digital camera and ToupView software (v3.7, ToupTek Photonics; Hangzhou, China).

2.2.4. Water holding capacity

Water holding capacity was measured for the starches according to the AACC-I method 56-20.01 ("Physical Modification of Food Starch Functionalities AACC International method 56-20.01," 1999), with modification to accommodate 1.0 g of sample to account for laboratory equipment available. The calculation was also modified to better reflect the amount of water the starches could hold. All samples were analyzed in triplicate.

$$\text{Water holding capacity} = \frac{(\text{Weight of hydrated starch}) - (\text{Weight of dry starch})}{(\text{Weight of dry starch})}$$

$$= g\ H_2O/g drystarch$$

2.2.5. Non-cold-set starch-protein dough preparation

The starch-protein isolate doughs were prepared at 47%(w/w). The levels of protein present in the dry fraction consisted of 0, 30, 50 and 70%(w/w) with the remaining fraction being composed of one of the three starches TI, CM, or GCS. The dry components of the sample were weighed and put into a 50 mL round bottom plastic centrifuge tube and vortexed for 30 s while simultaneously mixing with a glass stir rod to ensure that the starch and protein were fully mixed. The appropriate amount of water heated to 40°C was then slowly added to the dry fraction while again being vortexed to ensure all the dry material was hydrated. The resulting dough was then removed from the centrifuge tube and placed on to a temperature-controlled stainless-steel table set to 40°C. The doughs were manually kneaded in a repeated folding pattern for 1 min until a uniform texture was reached. Doughs left at this stage were considered non-cold-set.

2.2.5.1. Cold-set starch –Protein formation. The doughs prepared in section 2.2.5 were then placed in cylindrical molds 20 mm in diameter and 3 or 6 mm in height depending on the experiment as specified in the following methods. Doughs were refrigerated for 24 h at 5°C followed by equilibration for 1 h at room temperature before further testing. The samples having undergone refrigeration were considered cold-set.

2.2.6. Texture profile analysis (TPA)

2.2.6.1. Non-cold-set dough. A modified dough puncture/uniaxial compression test was performed on 5 g dough samples prepared as stated in 2.2.5 before any setting period, to investigate the texture profile of the starch and protein doughs under working/manipulation conditions. The method was adapted from the Stable Micro Systems biscuit dough method and texture profile analysis (Stable Micro Systems, n.d.). The test was executed by placing the non-cold-set dough sample into a 30 mm cylindrical tube and then pressed evenly with a flat plunger to obtain a level surface. The puncture/compression was performed using a TA.XT2 texture analyzer (Stable Micro Systems, Texture Technologies Corp. Scarsdale, NY, USA) fitted with a 5 mm cylindrical probe and 30 kg load cell. The dough underwent two compression cycles to a depth of 10 mm, at a crosshead speed of 1.0 mm/s with 5 s rest between compressions. The data was recorded in Newtons and analyzed using Exponent software. The hardness, resilience and cohesiveness were the chosen parameters and are as defined below (Bourne, 2002). All samples were analyzed in triplicate.

Hardness (N) = Maximum peak force of the first compression

Resilience (%) = up stroke energy from the first compression/down stroke energy of the first compression

Cohesiveness (%) = area of work during the second compression/area of work during the first compression

Chewiness = Hardness x Cohesiveness x Springiness

(Where the springiness is the distance of the detected height of the second compression divided by the original compression distance).

2.2.6.2. Cold-set dough. Non-cold-set dough samples prepared as stated in section 2.2.5 were set into 20mmx6 mm cylindrical molds as stated in 2.2.5.1 The batch size for cold set samples was large enough to form at least two samples disks per sample. After the 24 h setting period and equilibration time, TPA was performed on cold-set sample disks using a TA.XT2 texture analyzer (Stable Micro systems, Texture Technologies Corp. Scarsdale, NY, USA) fitted with 75 mm cylindrical plate and 30 kg load cell. The samples were compressed to 75% of their original height at a crosshead speed of 1.00 mm/s with 5 s rest between compressions. The data were recorded in Newtons and analyzed using Exponent software. The hardness, cohesiveness, resilience and chewiness were the parameters investigated as stated above in section (2.2.6.1) (Bourne, 2002). All samples were analyzed in at least duplicate.

2.2.6.2.1. Small deformation rheology. Dough samples were prepared as stated in section 2.2.5 and were set into 20 mm × 3 mm cylindrical molds as stated in 2.2.5.1 After the 24 h setting period and equilibration, oscillatory shear strain tests were performed using a rotational rheometer (MRC 302, Anton Paar, Graz, Austria) fit with a 20 mm parallel plate geometry (PP20/S) with the top and bottom plates affixed with 600 grit sandpaper to avoid slip. The gap was set to 3 mm, and the apparatus was temperature-controlled using Peltier plates and hood (Anton Paar, Graz, Austria) at a set temperature of 25°C. The amplitude sweep was performed at a logarithmic rate from 0.001 to 200% strain as a constant frequency of 1.0 Hz. The data was analyzed using RheoCompass Software. The variables obtained were elastic modulus (G'), loss modulus (G"), shear stress and yield point (critical strain); where the G′ value deviates greater than 5% than the previous average (Monthe et al., 2019). All samples were analyzed in triplicate.

2.2.7. Attenuated total reflectance- Fourier transform infrared spectroscopy

Starch and protein isolate were analyzed in both dry and non-cold-set dough forms prepared as stated in 2.2.5. The non-cold-set dough examined contained 0, 30 and 100% protein on dry matter base. The infrared spectra for the samples were obtained using a Fourier Transform Infrared Spectrometer (FTIR) (IRprestige 21-FTIR- Shimadzu Corp. Japan) fit with an attenuated total reflectance accessory (Pike Technologies, Madison, WI, USA). The scans were performed in the wavenumber range of 600–4000 cm^{-1} at a rate of 32 scans per spectra and resolution of 4 cm^{-1}. For the dry samples, background scans were taken with the crystal bare and for hydrated samples, water was used as the reference for subtraction. All spectra have undergone ATR correction (OMNIC Software, Thermo Scientific), to correct for the intensity of peaks due to the variation of the penetration depth of the evanescent wave with frequency. All samples were analyzed in triplicate.

2.2.8. Statistical analysis

GraphPad Prism 8.0 (GraphPad Software, SanDiego, CA, USA) was used to perform statistical analysis on all the data. Significance between samples was determined using one-way ANOVA followed by Tukey's Multiple Comparison Test.

3. Results and discussion

3.1. Differential Scanning Calorimetry

Differential Scanning Calorimetry (DSC) is a common technique used to investigate the gelatinization behavior of starch (Ratnayake and Jackson, 2008). The DSC investigation was performed to determine if unique structural elements were present which would have provided information as to why the starches have different rheological and textural properties. The onset temperature of gelatinization for waxy maize starch is normally between 65 and 67°C (Fredrikssona et al., 1998; W. Wang et al., 2017). However, starch modification can change the gelatinization temperature as internal bonds are strengthened and require more energy to break (Neelam et al., 2012). The starches TI, CM, GCS, have been modified to enhance their strength and physical properties but have also been pregelatinized (Neelam et al., 2012). There is a possibility that some structure can, however, remain in which an endothermic phase transition would be visible in the 25–120°C range (W. Wang et al., 2017). Fig. 1 shows the DSC thermograms for the three starches in which no thermal gelatinization endotherms from 30 to 100°C are present. This confirms that all the starches are fully gelatinized, and no crystalline structure remains. This trend was also seen by Chen and Jane (1994) in which different varieties of starch were modified to cold water swelling starches and similarly exhibited no gelatinization endotherms, as crystallinity was lost during the modification of the starches.

3.2. X-ray diffraction

X-ray diffraction is a technique used to investigate the crystallinity of starch. Native starch is made up of both crystalline and amorphous regions that organize and pack to provide unique x-ray diffraction patterns (Ratnayake and Jackson, 2008). The process of gelatinization causes loss of crystallinity and the X-ray diffraction pattern will demonstrate a uniform amorphous pattern (Ratnayake and Jackson, 2008). Fig. 2 shows powder X-ray diffraction spectra of each of the three starches all exhibiting a uniform amorphous pattern indicating no crystallinity. This supports the results observed by DSC, *i.e.,* no remaining crystallinity in the form of no endothermic events. Other studies have reported amorphous X-ray diffraction patterns for cold swelling waxy maize and for pregelatinized starch in which the modification resulted in the loss of crystallinity (J. Chen and Jane, 1994; Ratnayake and Jackson, 2006).

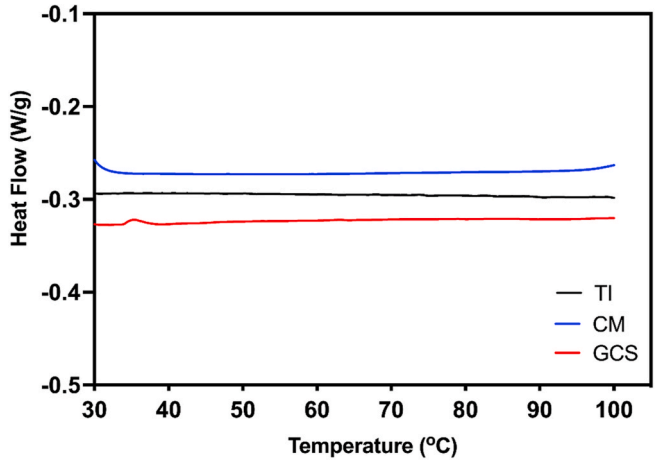

Fig. 1. DSC thermograms for starches, TI, CM, and GCS. Mean value of 2 scans.

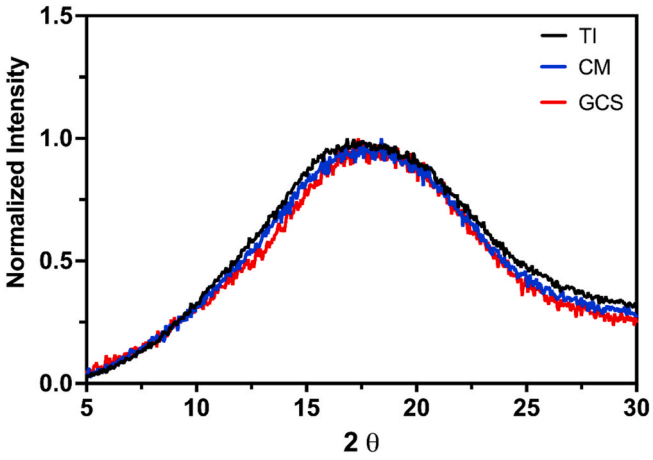

Fig. 2. X-Ray diffraction patterns for starches TI, CM, and GCS.

3.3. Microscopy

Bright-field microscopy images, with and without polarization were taken of the starches to provide visual indications as to the molecular arrangement inside the granules and the overall structure of the starch granules and suspensions. Iodine staining is a common technique used on starches to differentiate between genotypes in the starch (Evans et al., 2003). The bright-field images in Fig. 3 show purple to brown colouring for the majority of the sample background, which is characteristic of amylopectin-iodine interaction (Evans et al., 2003). However, for TI and GCS starch, dark blue granules are scattered throughout the sample which is the coloured complex formed when amylose reacts with iodine (Evans et al., 2003). The granular structure seen across the three starches also have differences. CM starch looks to have larger jagged structures with no distinguishable individual granules. TI and GCS look to be the most similar in their structure, having what looks like swollen granules packed together. GCS starch does appear to have more dense packing which could be attributed to the smaller swollen granule size. The bright-field images suggest that the starches are waxy and contain mainly amylopectin, with CM starch having an alternative structure due to its chemical modification.

The polarized images in Fig. 3 also provide some insight. In all of the starches, there are notable birefringence patterns with the Maltese crosses typical for native crystalline starch (X. Chen et al., 2017; Evans et al., 2003). A small amount of birefringence is expected, both CM and TI display only weak birefringence, while, GCS, has a much larger number of native granules distributed in the matrix. The greater degree of native granules for GCS may change the molecular organization and contribute to different textural characteristics.

3.4. Water holding capacity

The water holding capacity of the three starches can be seen in Fig. 4, where the TI starch has a water holding capacity of 9.78 ± 0.089 g H_2O/g dry starch, which is significantly lower than both CM and GCS having values of 13.28 ± 0.52 and 14.04 ± 0.12 g H_2O/g dry starch respectively. The water holding capacity of starch is dependent on the structure of the starches, which is influenced by the presence of amylose, amylopectin and the degree of crosslinking (Z. Q. Fu et al., 2012). Water absorption is highly influenced by the magnitude of inter- and intra-molecular bonds in the amorphous and crystalline structure of starch. In highly processed starches the structure is more disrupted by breaking inter and intramolecular hydrogen bonds which results in

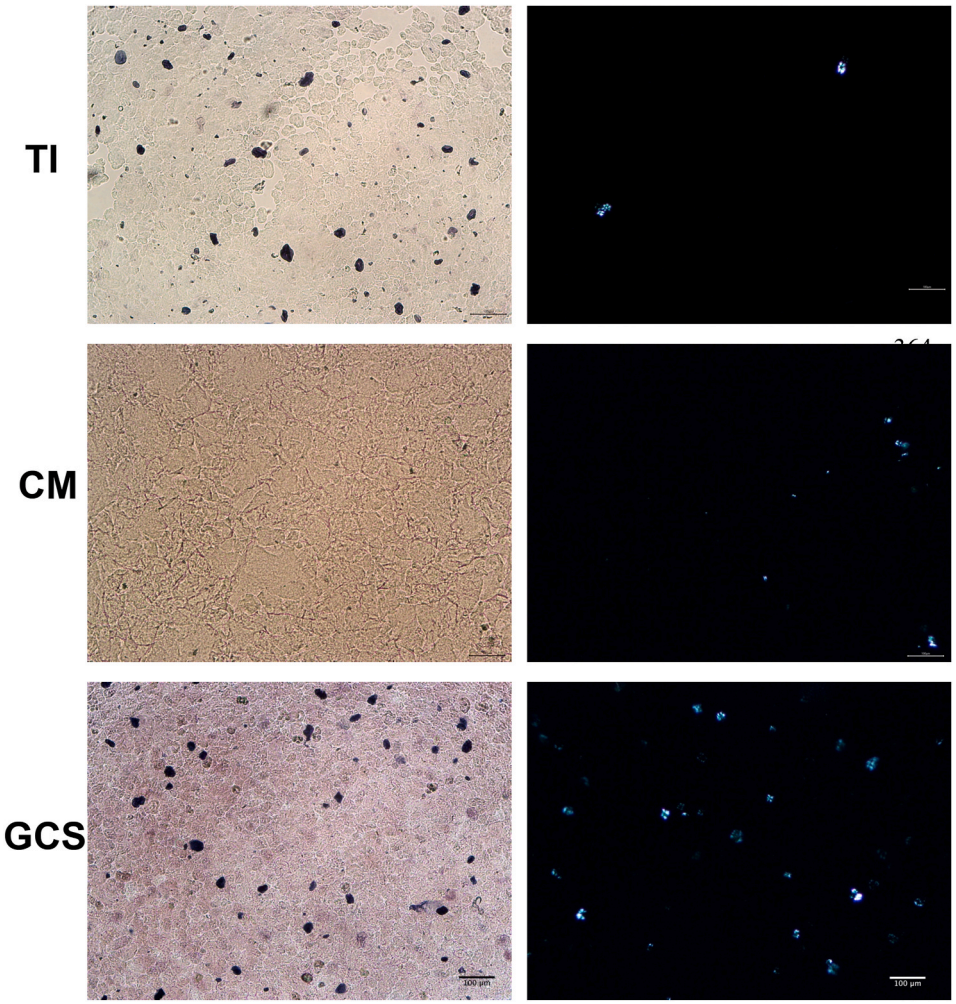

Fig. 3. Bright-field and corresponding polarized light microscopy of starches TI CM and GCS. Magnification bar corresponds to 100m.

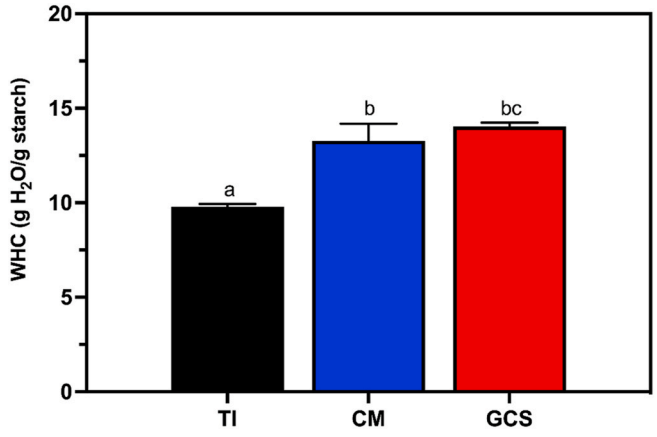

Fig. 4. Water holding capacity of the three starches, TI, CM, and GCS. All values reported are the mean ± SD. Mean values labelled with the same lowercase letter are not significantly different $P > 0.05$.

increased water absorption due to more exposed hydroxyl groups (Liu et al., 2017). This was seen for extruded pregelatinized starch with increasing degrees of moisture, in which the water absorption linearly increased due to more breakdown of structure (Liu et al., 2017). The degree of crosslinking also influences the hydration capacity, as an increased crosslinking reduces the swelling ability of the starch (Cui, 2005; N. Shah et al., 2016). This could indicate that CM is highly processes which would align with the microscopy findings in Fig. 3 of the jagged structures resulting in the starch having more exposed hydroxyl groups which increase its ability to hydrate. The high hydration also suggests there is limited crosslinking which likely restricts the ultimate strength of the starch matrix (Cui, 2005; Liu et al., 2017). As for GCS, the high hydration is typical of granular cold swelling starches with greater swelling capacity than normal pregelatinized starch, but these starches can maintain their overall structure due to the presence of the granules (Majzoobi et al., 2015; Xiong and Fei, 2017) The maintained granular structure of GCS can be seen in in Fig. 3. GCS did show increased presence of crystalline birefringence patterns (Fig. 3), but due to the observed high water holding it is likely that majority of the granules have an open structure and can absorb great amounts of water (Majzoobi et al., 2015). The low water holding capacity for TI starch is more unique and is likely related to the starch being prepared by "thermal inhibition" (Martin, 1967). The thermal inhibition process creates strong internal crosslinks and results in fewer exposed hydroxyl groups (Martin, 1967). The brightfield images (Fig. 3) suggest that there is less granular structure which aligns more with results seen for pre gelatinized starch which tend to have lower water holding capacity (Majzoobi et al., 2015). Some granular structure can however be seen, and with the suspected internal crosslinking, would lead to greater mechanical strength and lower content of free hydroxyl groups.

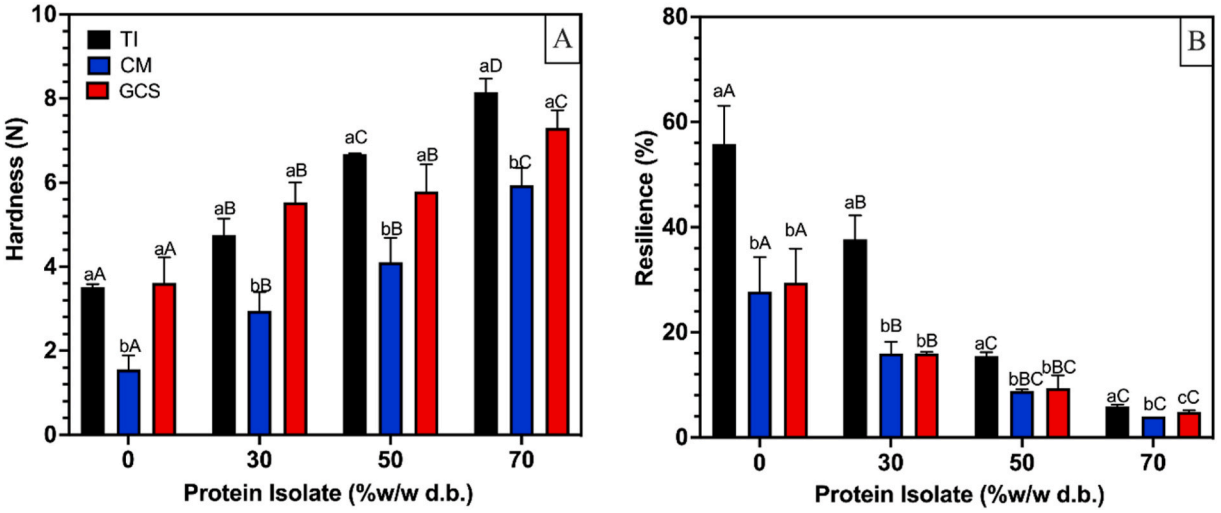

Fig. 5. Summary of TPA data of non-cold-set dough for starches TI, CM, and GCS with increasing amounts of protein (A) Hardness (B) Resilience. All values reported are the means ± SD. Dough values labelled with the same lower-case letter within the same protein concentration are not significantly different $P > 0.05$Mean values labelled with the same upper-case letter within the same starch variety are not significantly different $P > 0.05$.

3.5. Texture profile analysis of non-cold-set dough

The physical properties of non-cold-set starch-protein doughs immediately after preparation were analyzed to understand how the different starches compare as potential support matrices.

The hardness of the non-cold-set doughs (Fig. 5A) shows that across all concentrations, starches TI and GCS are both significantly harder than CM. The hardness is an important aspect to consider as it must be high enough to be self-supporting to withstand the possibility of other components being added in the future, such as, salt and acid which are known to weaken intermolecular bonds (Majzoobi et al., 2015; S. Wang and Copeland, 2015; W. Wang et al., 2017). The initial hardness of the CM starch is more comparable to that of a starch paste than dough. Majzoobi et al. (2015) performed a penetration texture test on 10%w/w pregelatinized starch pastes and obtained a firmness value of 1.35 N. The starches in this experiment were prepared to a concentration of 47 %w/w and CM starch exhibited an initial hardness value of only 1.55 N. The low hardness could be due to CM starch being more processed and having less granular structure (Fig. 3), which aligns with the greater water holding and thus less network strength (Cui, 2005; Liu et al., 2017). The greater hardness seen for GCS, on the other hand, is likely due to the intact granular structure (Fig. 3). GCS has visible starch granules and, even though the starch displayed the greatest water holding capacity (Fig. 4) the lower hydration level of the composite system, would limit the full swelling of the granules. This could then result in the starch granules emulating a particulate filler leading to a greater hardness (Gravelle et al., 2017). As for TI starch, the greater hardness observed can likely also be related to the lower hydration level of the composite resulting in more rigid granules. The microscopy image (Fig. 3) TI starch showed region of visible granules but also had areas of no definition. The greater observed hardness correlates to additional extensive internal crosslinking and limited exposed hydroxyl groups.

Fig. 5A shows that the addition of protein to all starches increased hardness. Due to the low hydration level and low heat, we assume that the protein is only acting as a filler, as the conditions do not support the formation of a protein gel network (Munialo et al., 2018). The starch is responsible for the majority of structure in the non-cold-set samples, creating a continuous phase for the protein particles to be embedded in. This is consistent with other work, in which the level of pregelatinized starch had to be great enough to have dough mimicking properties that provide the required viscosity and rigidity to prevent sedimentation of the other ingredients (Onyango et al., 2011).

Table 1
Non-cold-set and cold-set dough texture profile analysis cohesiveness data. All values reported are the means ± SD. Mean values labelled with the same lower-case letter within the same protein concentration and in the same subgroup (non-cold-set and cold-set) are not significantly different $P > 0.05$ Mean values labelled with the same upper-case letter within the same starch variety are not significantly different $P > 0.05$.

Cohesiveness (%)						
% Protein in Dry Fraction	TI	CM	GCS	TI	CM	GCS
	Non-Cold-Set Dough			Cold-Set Dough		
Mean 0 ± *SD*	89.5^{aA}	85.8^{aA}	88.1^{aA}	26.00^{aA}	30.9^{bA}	62.9^{cA}
	2.5	1.6	1.4	3.4	3.6	4.6
30	81.3^{aB}	76.8^{abAB}	74.2^{bAB}	39.3^{aB}	43.5^{abB}	68.1^{bAB}
	1.0	3.0	3.4	5.9	3.7	4.1
50	65.1^{aC}	69.5^{aBC}	66.0^{aBC}	42.2^{aB}	44.5^{aB}	60.4^{bA}
	4.0	8.7	4.1	3.3	6.4	6.8
70	56.3^{aD}	56.9^{aC}	56.3^{aC}	33.2^{aC}	38.8^{aAB}	30.7^{aC}
	0.6	5.2	4.1	4.5	11.5	4.4

From a theoretical standpoint, the hardness data suggests that the protein is acting as an active filler, as the addition of protein increases the hardness of the matrix (Dickinson, 2012). However, recent research on particle filled matrices proposed that there is an additional class known as a partially active filler (Gravelle et al., 2019). This alternative packing suggests that imperfect or partial adhesion occurs between the matrix and filler also providing structural matrix enhancements (Gravelle et al., 2019). As the ratio of protein to starch increases, the increased hardness is likely due crowding effects (Gravelle et al., 2017; Gravelle and Marangoni, 2021; Onyango et al., 2011; Ribotta et al., 2007).

The starches also provided great amounts of resilience and cohesiveness to the non-cold-set doughs as seen in Fig. 5B and Table 1. Resilience refers to how well a sample recovers from deformation in terms of speed and force, while cohesiveness is a measure of the strength of the internal bonds within the matrix and the extent of deformation that can be withstood before rupture (Chandra and Shamasundar, 2015; Fermin et al., 2006; Joshi et al., 2014; Radocaj et al., 2011.). In all cases, starch with no protein present had the greatest amount of resilience and cohesiveness as seen in Table 1 and Fig. 5B and the values continually decrease with added protein. Large values of cohesiveness and resilience show that the bonds holding the matrix together are stronger. Low values of cohesiveness and resilience, such as those seen with high concentrations of protein, result in weaker internal bonds and thus

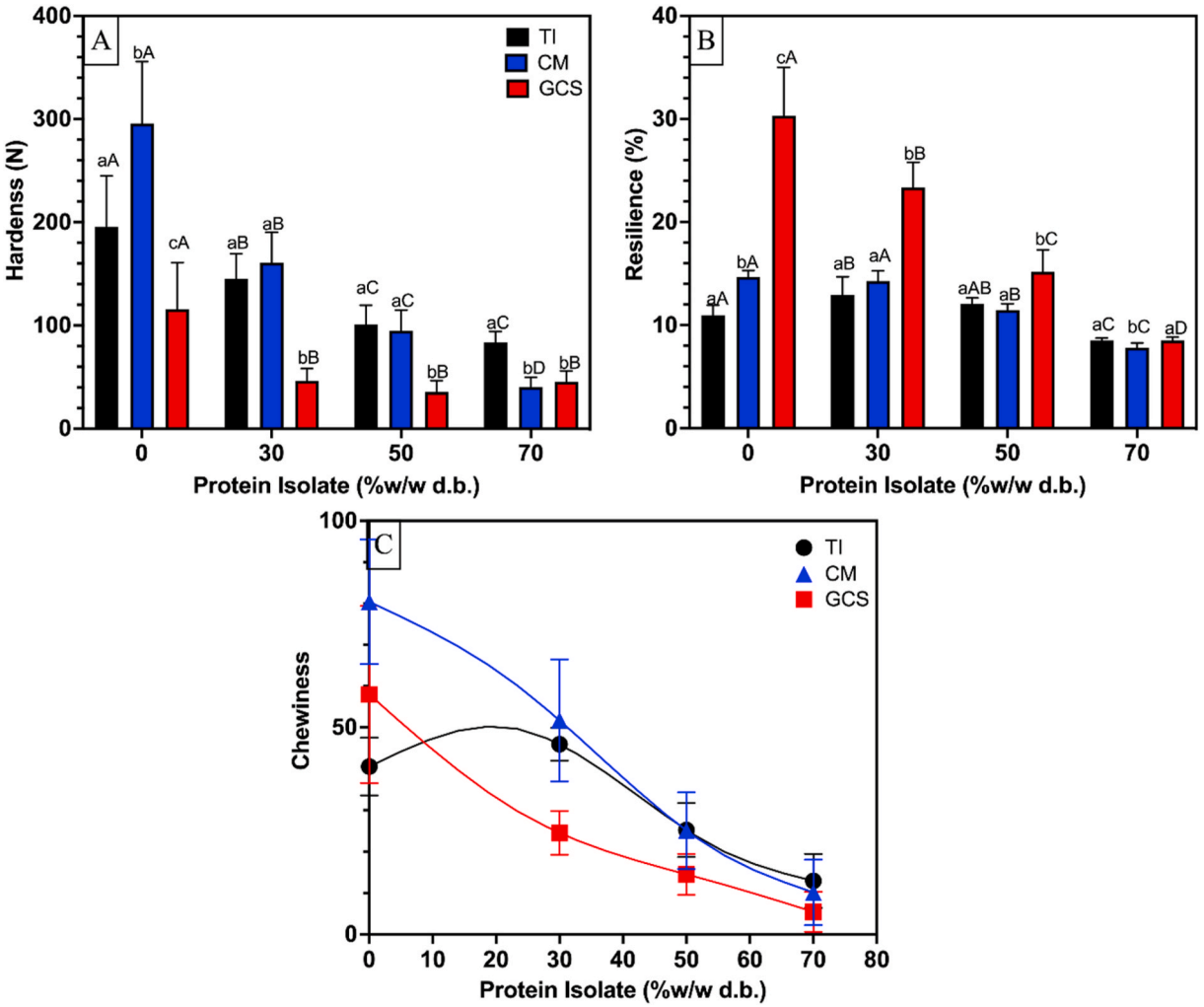

Fig. 6. Comparison of starches TI, CM, GCS texture profile analysis of cold-set starch-protein disks with increasing protein content. (a) Hardness (b) Resilience (c) Chewiness. All values reported are the means ± SD. Mean values labelled with the same lower-case letter within the same protein concentration are not significantly different $P > 0.05$ Mean values labelled with the same upper-case letter within the same starch variety are not significantly different $P > 0.05$.

greater degrees of deformation (M. Joshi et al., 2014). While the cohesiveness values remained similar between the starches, TI starch had significantly greater levels of resilience at all concentrations up to 70% protein. The greater resilience could be related to the lower water holding capacity and suspected strong internal crosslinking, creating a strong network that is not easily deformed. As the protein content increases it is important to note that the starch content would thus be decreasing. The ability for TI starch and pea protein to maintain a higher resilience indicates that the starch and protein are able to act synergistically to create a more elastic matrix.

3.6. Texture profile analysis of cold-set dough

Allowing the doughs to set at 5°C for 24 h after their formation, resulted in a greater reproducibility in all rheological measurements. This cold setting period allowed for the structures to set in a stable configuration, minimizing transient behavior and thus noise. The hardness of the cold-set doughs are shown in Fig. 6A. Results indicated that all starches increased in hardness after refrigeration at 5°C for 24 h, most probably due to starch retrogradation (Majzoobi et al., 2015). Across the varieties of starch, GCS was the softest at all protein concentrations up to 70%. The resilience data (Fig. 6B), as well as the cohesiveness data in Table 1, both displayed trends in which the values for GCS were significantly greater than the other starches. When comparing the resilience data between cold-set (Fig. 5B) and non-cold-set (Fig. 6B) dough, there were no significant differences observed. GCS starch is not able to form a cold-set mass, and instead remains a non-cold-set dough.

CM has the greatest initial hardness compared to starches TI and GCS in cold-set dough. This is related to the lack of granular structure which would enable the amylose and amylopectin to reorganize and retrograde easier, resulting in grater hardness. However, the responses to the addition of protein are different. The addition of protein resulted in the greatest initial decreases in hardness of the CM and GCS starches at 45.71% and 59.87% respectively, while TI resulted in the smallest decrease of only 25.71%. The large changes in hardness observed for CM and GCS suggest that the protein is interfering with starch intermolecular bonds to a greater extent than in TI starch, which is, in turn, is influencing the retrogradation process (Ribotta et al., 2007).

The greater chewiness and resilience of TI starch suggest a unique interaction (Fig. 6 B, C), where the addition of 30% protein resulted in a significant increase from initial values. The matrix strength-enhancing effect suggests that the protein is acting as an active filler and thus having strong interactions with the starch matrix. It is possible that the interaction could be related to the unique structure of thermally inhibited starch. TI starch has the lowest water holding capacity but one of the greatest hardness values, which has been related to the strong internal crosslinking and limited exposed and hydroxyl groups (Martin,

1967). It is possible that TI starch which would require less water to form a stable starch matrix, leaving more water initially available for the protein to form an alternative conformation that would favour interaction with TI starch during the setting period. This unique result is not seen for the other starches, as both GCS and CM display trends for passive fillers in which hardness, chewiness and resilience continually decrease with an increasing amount of added protein. This trend is most common and was also seen by Ribotta et al. (2007) where soy protein addition to a wheat starch gel decreased chewiness and hardness. It has also been reported by other authors that protein can act as a passive filler, disrupting the ability of the starch to reorganize during retrogradation (M. Joshi et al., 2014; Ribotta et al., 2007; H. Yang et al., 2004).

Overall, the TPA of the non-cold-set and cold-set doughs suggests that when initially mixed, protein addition enhances the hardness of starch, while decreasing resilience and cohesiveness. But, upon cold setting and starch retrogradation, the overall sample hardness increases dramatically. Protein incorporation in retrograded starch decreases hardness, cohesiveness and resilience as the protein particles behave as passive fillers.

3.7. Small deformation rheology

3.7.1. Amplitude sweep

Small deformation rheology was used to further investigate the structure of the cold-set starch-protein samples. The storage modulus (G′) reflects the elastic component of the sample while the loss modulus (G″) reflects the viscous portion. The yield point, or limit of the linear viscoelastic region (LVR) of material is a useful characteristic which is a function of the nature, strength and range and of interactions present. The yield point is equal to the shear strain, or stress, at which the G′ becomes strain dependent. For this investigation, it was determined that yield point could be identified when the G′ decreases by more than 5% from the G' of the LVR (Monthe et al., 2019).

The complete oscillatory sweeps for the three starches without protein, and with 30% protein, can be seen in Fig. 7A and B, respectively. In both Fig. 7A and B it is evident that the GCS starch is distinctly different than the other two starches, in which there is no crossover of the G′ with the G″, meaning, that the elastic component is constantly greater than the viscous component. Similar results were observed for freshly

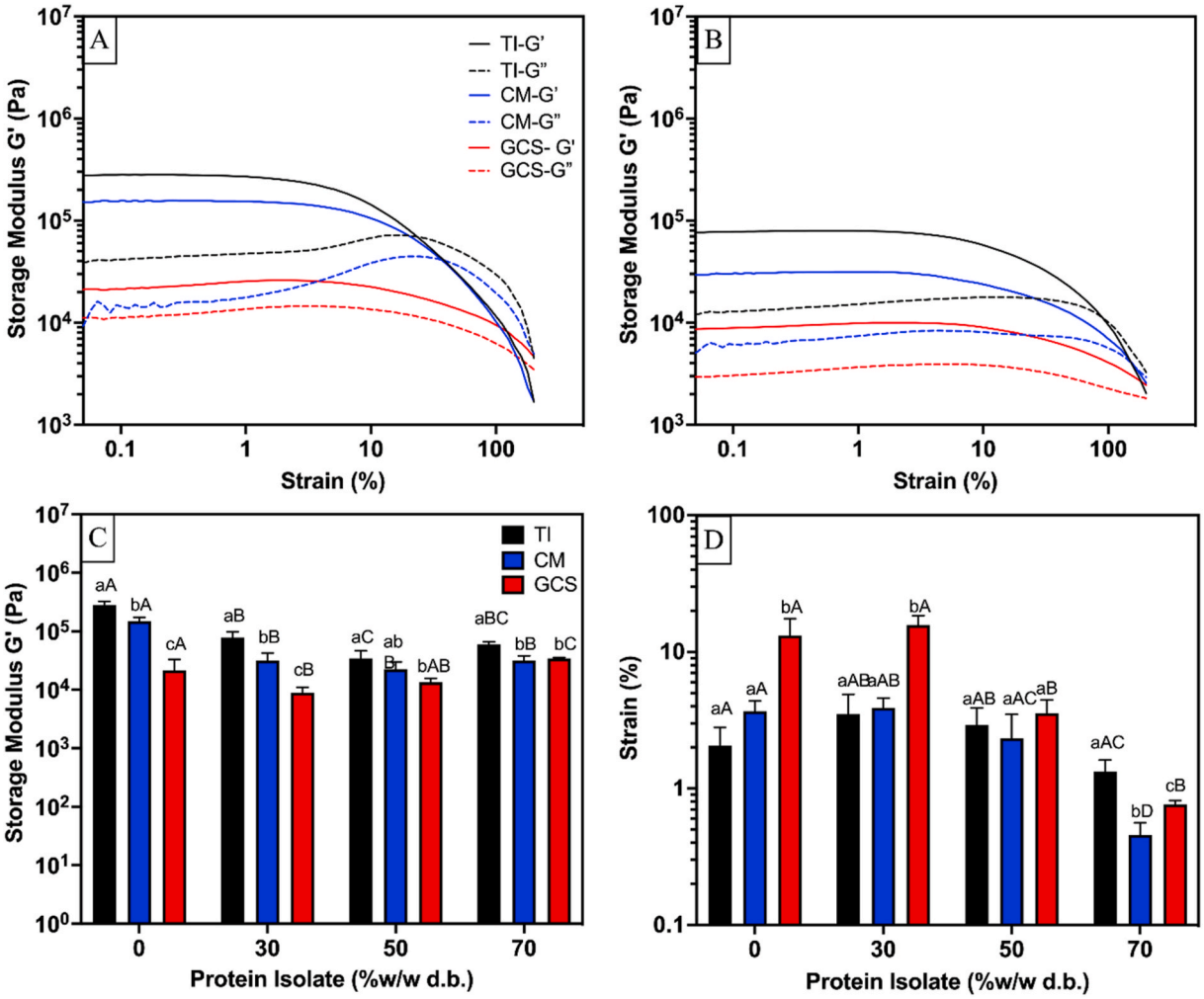

Fig. 7. Small deformation rheology of the cold-set dough samples of three starches, TI, CM, and GCS, with pea protein. (a) Amplitude sweeps for Starch 100% and Protein 0% in dry fraction. (b) Amplitude sweeps for Starch 70% and Protein 30% in dry fraction. (c) Summary of elastic modulus taken at 0.1% strain during the amplitude sweep for increasing amounts of protein. (d) Summary of the yield point taken from when the G′ deviated greater than 5% from the average. All values reported are the means ± SD. Mean values labelled with the same lower-case letter within the same protein concentration are not significantly different $P > 0.05$. Mean values labelled with the same upper-case letter within the same starch variety are not significantly different $P > 0.05$.

prepared starch and wheat doughs in which the G′ was always greater than G" (Z. Fu et al., 2016). This suggests that the GCS starch is not able to set into a solid structure but instead, remains a viscoelastic non-cold-set dough. These results further support the evidence observed in our TPA testing of the cold-set dough, in which GCS had significantly lower hardness and higher resilience. Starches TI and CM have similar oscillatory curves at the concentrations reported in Fig. 7A and B, but TI starch had significantly higher values for the G' and G".

Fig. 7C summarizes the effect of protein addition on the storage modulus of the three starches. The general trend is consistent across all starches in which, the addition of protein reduced the storage modulus. These results agree with our TPA data for cold-set dough suggesting that starch concentration is responsible for the overall apparent gel strength and the addition of protein disrupts the network. At the high end of the protein content, there some small increases in the G', but are likely attributed to the particle-filled matrix reaching the closed pack limit. Overall, TI starch, had the highest storage modulus for all protein contents, compared to starches CM and GCS (Fig. 7C). This indicates that TI starch can store greater amounts of elastic energy during deformation and displays more solid-like behaviour.

Additionally, the effect of protein on the length of the linear viscoelastic region (LVR) can be appreciated in Fig. 7C. The end of the LVR corresponds to the yield point, which provides information as to the amount of stress or strain a material can withstand, before reaching the critical level to cause irreversible deformation (TA Instruments, n.d.). No changes to the yield point upon the addition of protein up to 50%, were observed for CM and TI starch. This result is unexpected as, we see decreases in G′ and hardness with the addition of protein and would expect the addition of protein to affect the yield point. The constant gel strength could be related to CM being chemically cross-linked and TI also having existing crosslinking from the starch dehydration process. The additional crosslinking between the starch molecules would prevent the protein from causing any significant changes to the overall strength of the structure (N. Shah et al., 2016). The decrease in the width of the LVR at 70% protein can be linked to the lower starch content, and the protein-protein interactions not being able to compensate for the loss in starch-starch interactions. For TI starch however, the greater G' values along with the LVR being independent of protein concentration suggests that starch in combination with the protein are more capable at maintaining the strength of the matrix.

3.7.2. *Stress-strain*

From the rheological analysis, the stress vs strain curves for the three starches with increasing protein were also investigated and are shown in Fig. 8. Cold-set TI starch (Fig. 8A) with 0% protein showed the most brittle structure across all of the starches reaching the highest stress and then drastically dropping at higher strain. The brittle nature of the 0% protein sample was similar for CM starch (Fig. 8B), but it did not have the same degree of deformation at high shear. The addition of protein to both TI and CM resulted in more ductile behavior across all protein concentrations. However, for TI starch at 30% protein, the ductile behavior was met with greater stress values than those seen for protein containing samples in CM. We suspect the result seen with TI starch can be attributed to the structure of the starch granules in coordination with the lower water holding capacity. The crosslinked structure would require less water to create strong starch-starch interaction thus

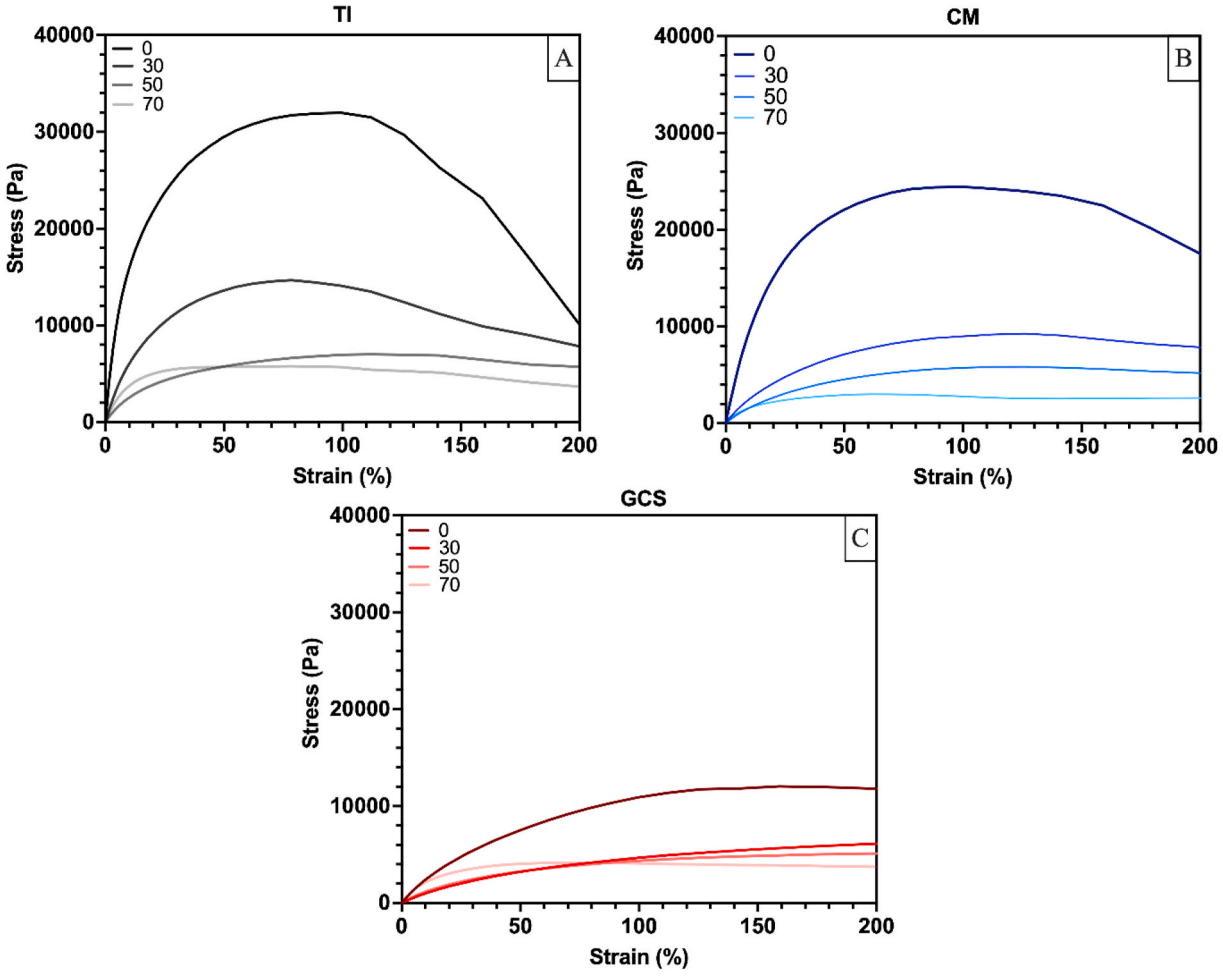

Fig. 8. Stress vs strain curves of starches with increasing protein for 0–70% A) TI starch B) CM starch C) GCS starch.

providing the network strength and the additional protein can also hydrate to a greater degree. The ability for TI starch to hold greater elastic energy in particular at 30% protein explains the increased resilience and chewiness observed for the cold-set samples. GCS starch (Fig. 8C) on the other hand was ductile at all protein concentration and had the lowest stress values which is consistent with the cold-set dough TPA data showing the sample remaining a viscoelastic dough.

3.8. Attenuated total reflectance- Fourier transform infrared spectroscopy

The traditional way of analyzing FTIR spectra entails the deconvolution of given regions into peaks that add up to the enveloping band. There are many drawbacks to this method, such as the possibility of over-deconvoluting the data by using too many peaks in the fit, inconsistent use of baselines, and the need for a very high S/N ratio in the data (S. Wang and Copeland, 2015). Although there are ways to address each of these issues (e.g. spectral smoothing) the process of deconvolution is highly dependent on the initial parameter evaluation (peak position, shape, width, etc.), making reproducibility hard to achieve by different users, even on the same dataset (Chittur, 1998; Yan et al., 2017). With this in mind, we decided to analyze the data in a way that minimizes the introduction of errors due to the data treatment itself and provides reproducible results.

Our approach involves subtracting peak intensities and comparing the difference in intensity between peaks for different samples. This comparative analysis relies on the fact that all the sample reps have identical composition and that across all samples the proportions of all components are the same.

The main vibrational modes that contribute to each of the analyzed peaks are summarized in Table 2. The assumption here is that band intensity differences correspond to differences in molecular changes and therefore molecular interactions, in accordance with Table 3. The drawback of this type of analysis is mainly the fact that although we will be able to see changes at the molecular level, we cannot pinpoint what is the cause of such change.

3.8.1. FTIR analysis of results

Amide I and II bands belong exclusively to the pea protein. Fig. 9 (black squares) shows that there is no significant difference between the three non-cold-set starch-protein doughs. There is however a difference with respect to the protein-only non-cold-set dough. This indicates the there is an effect on the protein due to the presence of starch, but it is not starch specific.

The PID between starch peaks (blue, green, and purple symbols), is the same for all the 2-component non-cold-set doughs (starch-protein), but there is a significant difference when compared to the starch-only non-cold-set doughs. This implies that there is an effect on the starch, due to the presence of the protein in the non-cold-set dough, but such an effect is not starch-specific. As such, there is no specific starch-starch interaction for any of the starches.

However, when looking at the PID of peaks that belong to the protein (AmI band) and the starch (1020 cm^{-1}), we can see that there is a significant difference in the case of the TI + F85 non-cold-set dough, with respect to the other non-cold-set starch-protein doughs (red circles). Therefore, there is a significant interaction between the pea protein and the specific starch TI, which does not occur (or occurs to a lesser extent) in the non-cold-set doughs made with GCS and CM starches. The same analysis was carried for PID between the AmII band of the protein, and the 1020 cm^{-1} peak of the starch. The data is not shown in Fig. 9 for clarity, but there was no significant difference between the non-cold-set doughs. This result further indicates that the protein-starch interaction in the TI + F85 dough involves not just any part of the protein, but the carbonyl group of the amide and could involve a conformational change within the protein.

Evidence for the interaction between the TI starch and F85F pea protein is supported in the rheological and texture analyses. At 30% protein, there is a significant increase in chewiness and resilience, which demonstrated that at that concentration there are changes in the matrix properties. Moreover, TI is the only starch at 30% protein to become ductile and maintain large amounts of matrix strength. The reasoning as to why this trend is only seen in TI, is likely related to the structure of the starch. The starch thermal inhibition process creates strong internal crosslinks and less exposed hydroxyl groups to bind with water but maintains a swollen granule structure. It is plausible that when mixed at the ratio with 30% protein, the protein is able to hydrate to a greater extent and possibly rearrange into a conformation that would yield an interaction between the starch and protein.

Table 2
Peak assignment for selected protein and starch features.

Band/peak	Belongs to	Vibrational modes
Amide I ~1635	Protein	Mostly C=O stretching vibrations of Amide groups
Amide II ~1540	Protein	CN stretching and NH bending (overlaps with amino acid side chain vibrations)
870–1050	Starch	C–O, C–C and C–H stretching modes in COH moieties (Capron et al., 2007).
1080	Starch	C–O–H stretching (Vicentini et al., 2005)
1150	Starch	C–O–C antisymmetric bridge stretching (Vicentini et al., 2005)

Table 3
Type of interaction probed based on peak intensity difference comparison.

Comparison	Type of interaction
Amide I | Amide II	Protein-Protein
Starch bands	Starch-Starch
AmI and AmII | Starch bands	Protein-Starch

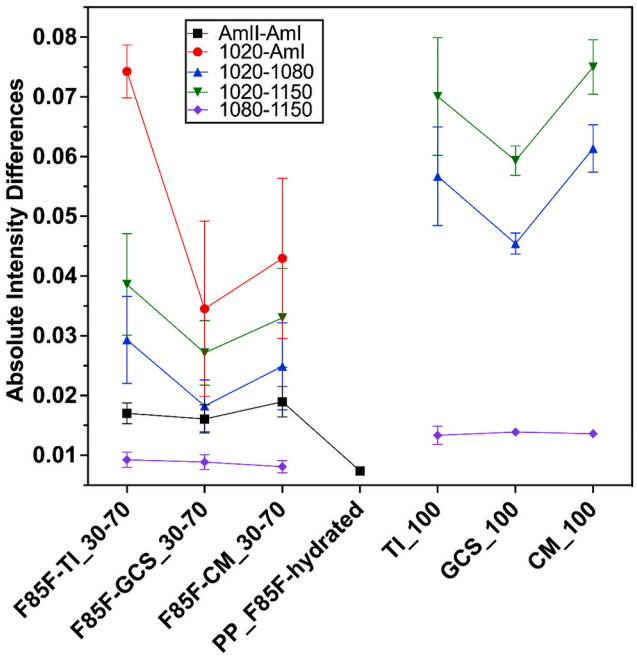

Fig. 9. Peak Intensity Deference (PID) for several combinations of protein and starch peaks for the starch-protein doughs made with the different starches and the F85 pea protein, as well as starch only and protein only doughs (x-axis). Error bars correspond to the standard deviation of at least three measurements. AmideII-AmideI (black squares), Amide I –1020 cm^{-1} peak (red circles), 1020 cm^{-1} – 1080 cm^{-1} (blue triangles), 1020 cm^{-1} – 1150 cm^{-1} (green triangles), 1080 cm^{-1} – 1150 cm^{-1} (purple diamonds).

Previous studies have shown that protein-starch interactions occur mainly via hydrogen bonds (J. Li, Yadav, and Li 2019; N. Yang, Ashton, and Kasapis 2015; Zhang et al., 2006; López-Barón et al., 2018; Mangavel et al., 2001; Guerrero, Kerry, and de la Caba 2014; Joshi et al., 2014b). In IR spectra, hydrogen bond interactions are usually studied in the hydroxyl-stretching region, found from 3650 to 3100 cm^{-1}. Unfortunately, since our samples are aqueous systems, background subtraction makes it difficult to study this region in our spectra. Therefore, although we cannot be certain, we speculate that the peptide's carbonyl (as represented in the IR Amide I band) undergoes a change such that there is an increase in the ability of the peptide to hydrogen bond with the specific TI starch.

4. Conclusion

The investigation of the three rapid swelling starches; TI, CM, and GCS, indicated that they were all amorphous based on the single broad X-ray diffraction peak and fully gelatinized as there were no endothermic events determined by DSC. They did, however, have a distinct microstructure with TI and GCS having swollen granules and CM exhibiting sharp jagged structures. The water holding capacity also differed with CM and GCS displaying a significantly greater water holding capacity than TI. In the non-cold-set and cold-set states, each of the starches provided different textural attributes. Overall, in noncold-set dough, the addition of protein increased hardness displaying properties of an active or partially active filler. TI and GCS had greater hardness values, while CM displayed more paste like properties. However, the resilience of the non-cold-set TI starch was significantly greater at all protein concentrations.

After tempering at 5°C for 24 h, GCS starch did not set into a solid structure, remaining as a fluid dough. The sample had low hardness, high resilience and no cross-over of G' and G".

The hardness and storage modulus for cold-set CM and TI starch followed the same trend in which the protein acted as an inactive filler continually decreasing sample hardness. The addition of protein also made the samples more ductile as indicated by the stress vs strain curves.

However, for TI starch, the resilience and chewiness, had a unique result in which, protein addition at 30%, significantly increased the values from the starch only controls. Additionally, FTIR analysis using Peak Intensity Differences of the three starches with pea protein at 30% provided the most significant evidence of an interaction. In comparing the Amide I peak to the starch peak at 1020 cm^{-1}, TI starch and pea protein were significantly different from the samples with CM and GCS. The result suggested that there was a significant interaction occurring between TI starch and pea protein that was not occurring with CM or GCS. Overall, we determined that the textural and mechanical properties can be modulated with the addition of protein and that TI and pea protein show evidence of interactions which may enhance its potential for use in a novel meat analogue.

CRediT authorship contribution statement

Stacie Dobson: designed and carried out experiments, analyzed data, Formal analysis, Data curation, prepared the manuscript for publication. **Thamara Laredo:** carried out the FTIR experiments and analysis related to the FTIR, Formal analysis, as well as editing the manuscript, Writing – review & editing. **Alejandro G. Marangoni:** obtained funding for the project, Funding acquisition, supervised SM, Supervision, designed experiments and edited the manuscript, Writing – review & editing.

Declaration of competing interest

The authors declare the following financial interests/personal relationships which may be considered as potential competing interests:

Alejandro Marangoni reports financial support was provided by Natural Sciences and Engineering Research Council of Canada.

Acknowledgments

The Authors would like to acknowledge the National Sciences and Engineering Research Council for funding this research.

References

Alam, M.S., Kaur, J., Khaira, H., Gupta, K., 2016. Extrusion and extruded products: changes in quality attributes as affected by extrusion process parameters: a review. Crit. Rev. Food Sci. Nutr. 56 (3), 445–473. https://doi.org/10.1080/10408398.2013.779568.

Ashogbon, A.O., Akintayo, E.T., 2014. Recent trend in the physical and chemical modification of starches from different botanical sources: a review. Starch Staerke 66 (1–2), 41–57. https://doi.org/10.1002/star.201300106.

Bourne, M., 2002. Food Texture and Viscosity, second ed. Academic Press, New York.

Bühler, J.M., Schlangen, M., Möller, A.C., Bruins, M.E., van der Goot, A.J., 2022. Starch in plant-based meat replacers: a new approach to using endogenous starch from cereals and legumes. Starch - Stärke 74 (1–2), 2100157. https://doi.org/10.1002/STAR.202100157.

Capron, I., Robert, P., Colonna, P., Brogly, M., Planchot, V., 2007. Starch in rubbery and glassy states by FTIR spectroscopy. Carbohydr. Polym. 68 (2), 249–259. https://doi.org/10.1016/j.carbpol.2006.12.015.

Chandra, M.V., Shamasundar, B.A., 2015. Texture profile Analysis and functional properties of gelatin from the skin of three species of fresh water fish. Int. J. Food Prop. 18 (3), 572–584. https://doi.org/10.1080/10942912.2013.845787.

Chen, J., Jane, J., 1994. Properties of granular cold-water-soluble starches prepared by alcoholic-alkaline treatments'. Retrieved from. https://pdfs.semanticscholar.org/5e95/cbb68a1b9dd5e73899ea9485582b75c63c00.pdf.

Chen, X., He, X.-W., Zhang, B., Fu, X., Jane, J., Huang, Q., 2017. Effects of adding corn oil and soy protein to corn starch on the physicochemical and digestive properties of the starch. Int. J. Biol. Macromol. 104, 481–486. https://doi.org/10.1016/J.IJBIOMAC.2017.06.024.

Chittur, K.K., 1998. FTIR/ATR for protein adsorption to biomaterial surfaces. Biomaterials 19 (4), 357–369. https://doi.org/10.1016/S0142-9612(97)00223-8.

Cui, S.W., 2005. FOOD CARBOHYDRATES Chemistry, Physical Properties, and Applications. Taylor & Francis Group. https://doi.org/10.1074/jbc.270.35.20629.

De Bakker, E., Dagevos, H., 2012. Reducing meat consumption in today's consumer society: questioning the citizen-consumer gap. J. Agric. Environ. Ethics 25, 877–894. https://doi.org/10.1007/s10806-011-9345-z.

De Castro, A., Marketing Manager, S.R., 2015. NOVATION ® Functional Native Starches Non-GMO Project Verified.

Dickinson, E., 2012. Emulsion gels: the structuring of soft solids with protein-stabilized oil droplets. Food Hydrocolloids 28 (1), 224–241. https://doi.org/10.1016/j.foodhyd.2011.12.017.

Donmez, D., Pinho, L., Patel, B., Desam, P., Campanella, O.H., 2021. Characterization of starch–water interactions and their effects on two key functional properties: starch gelatinization and retrogradation. Curr. Opin. Food Sci. 39, 103–109. https://doi.org/10.1016/J.COFS.2020.12.018.

Evans, A., McNish, N., Thompson, D.B., 2003. Polarization colors of lightly iodine-stained maize starches for amylose-extender and related genotypes in the W64A inbred line. Starch Staerke 55 (6), 250–257. https://doi.org/10.1002/star.200390052.

Fermin, B.C., Hahm, T.S., Radinsky, J.A., Kratochvil, R.J., Hall, J.E., Lo, Y.M., 2006. Effect of proline and glutamine on the functional properties of wheat dough in winter wheat varieties. J. Food Sci. 70 (4), E273–E278. https://doi.org/10.1111/j.1365-2621.2005.tb07183.x.

Fredrikssona, H., Silveriob, J., Andemon, R., Eliassonb, A.-C., Amanta, P., 1998. The influence of amylose and amylopectin characteristics on gelatinization and retrogradation properties of different starches. Carbohydrate Polywm 35.

Fu, Z., Che, L., Li, D., Wang, L., Adhikari, B., 2016. Effect of partially gelatinized corn starch on the rheological properties of wheat dough. LWT - Food Sci. Technol. 66, 324–331. https://doi.org/10.1016/J.LWT.2015.10.052.

Fu, Z.Q., Wang, L.J., Li, D., Adhikari, B., 2012. Effects of partial gelatinization on structure and thermal properties of corn starch after spray drying. Carbohydr. Polym. 88 (4), 1319–1325. https://doi.org/10.1016/j.carbpol.2012.02.010.

Gravelle, A.J., Barbut, S., Marangoni, A.G., 2015. Influence of particle size and interfacial interactions on the physical and mechanical properties of particle-filled myofibrillar protein gels. RSC Adv. 5 (75), 60723–60735. https://doi.org/10.1039/C5RA07254A.

Gravelle, A.J., Barbut, S., Marangoni, A.G., 2017. Food-grade filler particles as an alternative method to modify the texture and stability of myofibrillar gels. Sci. Rep. 7 (1), 1–16. https://doi.org/10.1038/s41598-017-11711-1.
Gravelle, A.J., Marangoni, A.G., 2021. The influence of network architecture on the large deformation and fracture behavior of emulsion-filled gelatin gels. Food Struct. 100193. https://doi.org/10.1016/j.foostr.2021.100193.
Gravelle, A.J., Nicholson, R.A., Barbut, S., Marangoni, A.G., 2019. Considerations for readdressing theoretical descriptions of particle-reinforced composite food gels. Food Res. Int. 122, 209–221. https://doi.org/10.1016/j.foodres.2019.03.070.
Guerrero, P., Kerry, J.P., de la Caba, K., 2014. FTIR characterization of protein-polysaccharide interactions in extruded blends. Carbohydr. Polym. 111, 598–605. https://doi.org/10.1016/j.carbpol.2014.05.005.
Hampton, J.O., Hyndman, T.H., Allen, B.L., Fischer, B., 2021. Animal harms and food production: informing ethical choices. Animals : An Open Access J. MDPI 11 (5). https://doi.org/10.3390/ANI11051225.
Joshi, M., Aldred, P., Panozzo, J.F., Kasapis, S., Adhikari, B., 2014. Rheological and microstructural characteristics of lentil starchelentil protein composite pastes and gels. Food H (35), 226–237. https://doi.org/10.1016/j.foodhyd.2013.05.016.
Joshi, V., Kumar, S., 2015. Meat Analogues: plant based alternatives to meat products- A review. Int. J. Food Ferment. Technol. 5 (2), 107. https://doi.org/10.5958/2277-9396.2016.00001.5.
Lazaridou, A., Duta, D., Papageorgiou, M., Belc, N., Biliaderis, C.G., 2007. Effects of hydrocolloids on dough rheology and bread quality parameters in gluten-free formulations. J. Food Eng. 79 (3), 1033–1047. https://doi.org/10.1016/j.jfoodeng.2006.03.032.
Li, J.-Y., Yeh, A.-I., Fan, K.-L., 2006. Gelation Characteristics and Morphology of Corn Starch/soy Protein Concentrate Composites during Heating. https://doi.org/10.1016/j.jfoodeng.2005.12.043.
Li, J., Yadav, M.P., Li, J., 2019. Effect of different hydrocolloids on gluten proteins, starch and dough microstructure. J. Cereal. Sci. 87, 85–90. https://doi.org/10.1016/j.jcs.2019.03.004.
Liu, Y., Chen, J., Luo, S., Li, C., Ye, J., Liu, C., Gilbert, R.G., 2017. Physicochemical and structural properties of pregelatinized starch prepared by improved extrusion cooking technology. Carbohydr. Polym. 175, 265–272. https://doi.org/10.1016/j.carbpol.2017.07.084.
López-Barón, N., Sagnelli, D., Blennow, A., Holse, M., Gao, J., Saaby, L., Vasanthan, T., 2018. Hydrolysed pea proteins mitigate in vitro wheat starch digestibility. Food Hydrocolloids 79, 117–126. https://doi.org/10.1016/j.foodhyd.2017.12.009.
Loveday, S.M., 2020. Plant protein ingredients with food functionality potential. Nutr. Bull. 45 (3), 321–327. https://doi.org/10.1111/NBU.12450.
Majzoobi, M., Kaveh, Z., Blanchard, C.L., Farahnaky, A., 2015. Physical properties of pregelatinized and granular cold water swelling maize starches in presence of acetic acid. Food Hydrocolloids 51, 375–382. https://doi.org/10.1016/j.foodhyd.2015.06.002.
Mangavel, C., Barbot, J., Popineau, Y., Guéguen, J., 2001. Evolution of wheat gliadins conformation during film formation: a fourier Transform infrared study. J. Agric. Food Chem. 49 (2), 867–872. https://doi.org/10.1021/jf0009899.
Mariotti, M., Lucisano, M., Pagani, M.A., Ng, P.K.W., 2009. The role of corn starch, amaranth flour, pea isolate, and Psyllium flour on the rheological properties and the ultrastructure of gluten-free doughs. Food Res. Int. 42, 963–975. https://doi.org/10.1016/j.foodres.2009.04.017.
Martin, I., 1967. Crosslinking of starch by alkaline roasting. J. Appl. Polym. Sci. 11 (7), 1283–1288. https://doi.org/10.1002/app.1967.070110724.
Mattice, K.D., Marangoni, A.G., 2020a. Comparing methods to produce fibrous material from zein. Food Res. Int. 128, 108804 https://doi.org/10.1016/j.foodres.2019.108804.
Mattice, K.D., Marangoni, A.G., 2020b. Evaluating the use of zein in structuring plant-based products. Curr. Res. Food Sci. https://doi.org/10.1016/j.crfs.2020.03.004.
Monthe, O.C., Grosmaire, L., Nguimbou, R.M., Dahdouh, L., Ricci, J., Tran, T., Ndjouenkeu, R., 2019. Rheological and textural properties of gluten-free doughs and breads based on fermented cassava, sweet potato and sorghum mixed flours. Lebensm. Wiss. Technol. 101, 575–582. https://doi.org/10.1016/j.lwt.2018.11.051.
Munialo, C.D., Euston, S.R., De Jongh, H.H.J., 2018. Proteins in food processing protein gels. https://doi.org/10.1016/B978-0-08-100722-8.00020-6.
Neelam, K., Vijay, S., Lalit, S., 2012. Various techniques for the modification of starch and the applications of its derivatives. Int. Res. J. Pharm. 3 (5), 25–31.
Nijdam, D., Rood, T., Westhoek, H., 2012. The price of protein: review of land use and carbon footprints from life cycle assessments of animal food products and their substitutes. Food Pol. 37, 760–770. https://doi.org/10.1016/j.foodpol.2012.08.002.
Oguntoyinbo, S.I., Taylor, J.R.N., Taylor, J., 2018. Comparative functional properties of kafirin and zein viscoelastic masses formed by simple coacervation at different acetic acid and protein concentrations. J. Cereal. Sci. 83 (June), 16–24. https://doi.org/10.1016/j.jcs.2018.07.008.
Onyango, C., Mutungi, C., Unbehend, G., Lindhauer, M.G., 2011. Rheological and textural properties of sorghum-based formulations modified with variable amounts of native or pregelatinised cassava starch. LWT - Food Sci. Technol. 44 (3), 687–693. https://doi.org/10.1016/j.lwt.2010.08.019.
Physical Modification of Food Starch Functionalities AACC International Method 56-20.01, 1953, 1999.
Radocaj, O., Dimic, E., Vujasinovic, V., 2011. Optimization of the texture of fat-based spread containing hull-less pumpkin (Cucurbita pepo L.) seed press-cake. Acta Period. Technol. 42 (42), 131–143. https://doi.org/10.2298/APT1142131R.
Ratnayake, W.S., Jackson, D.S., 2006. A new insight into the gelatinization process of native starches q. https://doi.org/10.1016/j.carbpol.2006.06.025.
Ratnayake, W.S., Jackson, D.S., 2008. Chapter 5 starch gelatinization. Adv. Food Nutr. Res. 55 (8), 221–268. https://doi.org/10.1016/S1043-4526(08)00405-1.
Ribotta, P.D., Colombo, A., León, A.E., Añón, M.C., 2007. Effects of soy protein on physical and rheological properties of wheat starch. Starch - Stärke 59 (12), 614–623. https://doi.org/10.1002/star.200700650.
Ryan, K., Brewer, M., 2007. In situ examination of starch granule-soy protein and wheat protein interactions. Food Chem. 104 (2), 619–629. https://doi.org/10.1016/j.foodchem.2006.12.037.
Shah, M., Thomas, D.J., Chiu, C.-W., Jeffcoat, R., JHanchett, D.J., 1998. THERMALLYINHIBITED pregelatnzed granular starches and flours and process forther production. https://doi.org/10.7868/s0044457x13090079.
Shah, N., Mewada, R.K., Mehta, T., 2016. Crosslinking of starch and its effect on viscosity behaviour. Rev. Chem. Eng. 32 (2), 265–270. https://doi.org/10.1515/revce-2015-0047.
(n.d.) Stable Micro Systems. Bakery product texture analysis | stable Micro systems, Retrieved April 27, 2020, from. https://www.stablemicrosystems.com/BakeryProductTesting.html.
A Instruments. (n.d.). Rheological Techniques for Yield Stress Analysis.
Tattiyakul, J., Rao, M.A., 2000. Rheological behavior of cross-linked waxy maize starch dispersions during and after heating. Carbohydr. Polym. 43 (3), 215–222. https://doi.org/10.1016/S0144-8617(00)00160-0.
Taylor, J., Taylor, J.R.N., 2018. Making Kafirin, the sorghum prolamin, into a viable alternative protein source. JAOCS, J. Am. Oil Chemists' Soc. 95 (8), 969–990. https://doi.org/10.1002/aocs.12016.
(n.d.) Texture Technologies. Texture profile Analysis | texture Technologies, Retrieved April 27, 2020, from. https://texturetechnologies.com/resources/texture-profile-analysis.
Vicentini, N.M., Dupuy, N., Leitzelman, M., Cereda, M.P., Sobral, P.J.A., 2005. Prediction of cassava starch edible film properties by chemometric analysis of infrared spectra. Spectrosc. Lett. 38 (6), 749–767. https://doi.org/10.1080/00387010500316080.
Wang, J., Zhao, S., Min, G., Qiao, D., Zhang, B., Niu, M., Lin, Q., 2021. Starch-protein interplay varies the multi-scale structures of starch undergoing thermal processing. Int. J. Biol. Macromol. 175, 179–187. https://doi.org/10.1016/j.ijbiomac.2021.02.020.
Wang, S., Copeland, L., 2015. Effect of acid hydrolysis on starch structure and functionality: a review. Crit. Rev. Food Sci. Nutr. 55 (8), 1081–1097. https://doi.org/10.1080/10408398.2012.684551.
Wang, W., Zhou, H., Yang, H., Zhao, S., Liu, Y., Liu, R., 2017. Effects of salts on the gelatinization and retrogradation properties of maize starch and waxy maize starch. Food Chem. 214, 319–327. https://doi.org/10.1016/j.foodchem.2016.07.040.
Wang, Y., Chen, L., 2012. Fabrication and characterization of novel assembled prolamin protein nanofabrics with improved stability, mechanical property and release profiles. J. Mater. Chem. 22 (40), 21592. https://doi.org/10.1039/c2jm34611g.
Xiong, H., Fei, P., 2017. Critical reviews in food science and nutrition physical and chemical modification of starches: a review Zia-ud-Din, Hanguo Xiong & Peng Fei physical and chemical modification of starches: a review. https://doi.org/10.1080/10408398.2015.1087379.
Yan, Z., Li, Q., Zhang, P., 2017. Soy protein isolate and glycerol hydrogen bonding using two-dimensional correlation (2D-COS) attenuated total reflection fourier Transform infrared (ATR FT-IR) spectroscopy. Appl. Spectrosc. 71 (11), 2437–2445. https://doi.org/10.1177/0003702817710249.
Yang, H., Irudayaraj, J., Otgonchimeg, S., Walsh, M., 2004. Rheological study of starch and dairy ingredient-based food systems. Food Chem. (86), 571–578. https://doi.org/10.1016/j.foodchem.2003.10.004.
Yang, N., Ashton, J., Kasapis, S., 2015. The influence of chitosan on the structural properties of whey protein and wheat starch composite systems. Food Chem. 179, 60–67. https://doi.org/10.1016/j.foodchem.2015.01.121.
Zhang, X., Do, M.D., Hoobin, P., Burgar, I., 2006. The phase composition and molecular motions of plasticized wheat gluten-based biodegradable polymer materials studied by solid-state NMR spectroscopy. Polymer 47 (16), 5888–5896. https://doi.org/10.1016/j.polymer.2006.05.060.